

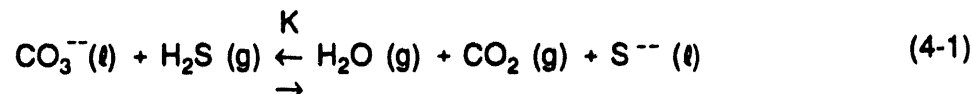
SECTION 4

THEORETICAL MODELING OF FACILITATED TRANSPORT

The steady-state data collected during the membrane experiments may be used to estimate parameters governing the facilitated transport of H₂S through the molten salt. A brief description of the facilitated transport concept and the process chemistry involved was provided in Section 1.1. Based on this understanding of the concept, approximate relationships may be developed to predict the flux rate of H₂S transport through a molten salt.

4.1 ANALYSIS OF STEADY-STATE DATA

The H₂S absorption and stripping reactions occurring on the two sides of a molten salt impregnated ceramic membrane are expressed by the reversible reaction given in Equation (1-1).



where K is a chemical equilibrium constant for the above reaction and is given by

$$K = \frac{[\text{S}^{--}] [\text{H}_2\text{O}] [\text{CO}_2]}{[\text{H}_2\text{S}] [\text{CO}_3^{--}]} \quad (4-2)$$

where

- S⁻⁻ = Molar concentration of S⁻⁻ ions in the liquid phase (gmole/cm³)
- CO₃⁻⁻ = Molar concentration of CO₃⁻⁻ ions in the liquid phase (gmole/cm³)
- H₂O = Molar concentration of water vapor in the gas phase expressed as partial pressure in atm
- CO₂ = Molar concentration of CO₂ in the gas phase expressed as partial pressure in atm
- H₂S = Molar concentration of H₂S in the gas phase expressed as partial pressure in atm
- K = Reaction equilibrium constant in atm.

The equilibrium constant, K, is a function of reaction temperature, T. Since the partial pressures of the reacting species, H₂O, CO₂, and H₂S, are different on the feed and sweep sides of the membrane, the concentrations of the sulfide and carbonate ions on the respective membrane

surfaces will be different at steady-state chemical equilibrium conditions. The differences in liquid phase concentrations on the two sides of a membrane will establish a concentration gradient within the liquid phase as shown schematically in Figure 4-1.

Since 1 mol of carbonate ion $[\text{CO}_3^{--}]$ produces 1 mol of sulfide ion $[\text{S}^{--}]$ by reacting with H_2S , according to Equation (4-1), the total molar concentration in the liquid phase is expected to be the same, regardless of the extent of reaction. For pure carbonate melt to begin with, the total molar concentration, C_T , gmoles/cm³, is given by

$$C_T = [\text{S}^{--}] + [\text{CO}_3^{--}]. \quad (4-3)$$

Any loss of salt by evaporation and presence of impurities in the salt is ignored in the above equation. The fraction of the sulfide ions $[\text{S}^{--}]$ at any position in the liquid phase may be expressed by X

$$X = [\text{S}^{--}] / C_T. \quad (4-4)$$

The corresponding fraction of carbonate ions is given by

$$1 - X = [\text{CO}_3^{--}] / C_T. \quad (4-5)$$

The equilibrium constant, K, may be expressed in terms of X and gas phase partial pressures

$$K = \frac{X \cdot p(\text{H}_2\text{O}) \cdot p(\text{CO}_2)}{(1-X) p(\text{H}_2\text{S})}. \quad (4-6)$$

The sulfide ion fraction in the melt at the feed side and sweep side membrane surfaces is then given by

$$X = \frac{K p(\text{H}_2\text{S})}{K p(\text{H}_2\text{S}) + p(\text{H}_2\text{O}) p(\text{CO}_2)}. \quad (4-7)$$

By substituting appropriate gas phase partial pressure values, Equation (4-7) can provide the sulfide ion fraction on the two sides of the membrane, x_{feed} and x_{sweep} .

The flux rate of sulfide ions, S^{--} , across the liquid phase depends on the diffusivity of sulfide ions in the liquid phase and the sulfide ion concentration gradient. The molar flux rate of gas phase H_2S across the liquid phase membrane by the reaction pathway is, in effect, provided by the molar flux rate of the sulfide ions across the liquid phase.

$$J_{\text{H}_2\text{S}} = \frac{D_{(\text{S}^{--})}}{\ell} \cdot A \cdot C_T \cdot (X_{\text{feed}} - X_{\text{sweep}}) \quad (4-8)$$

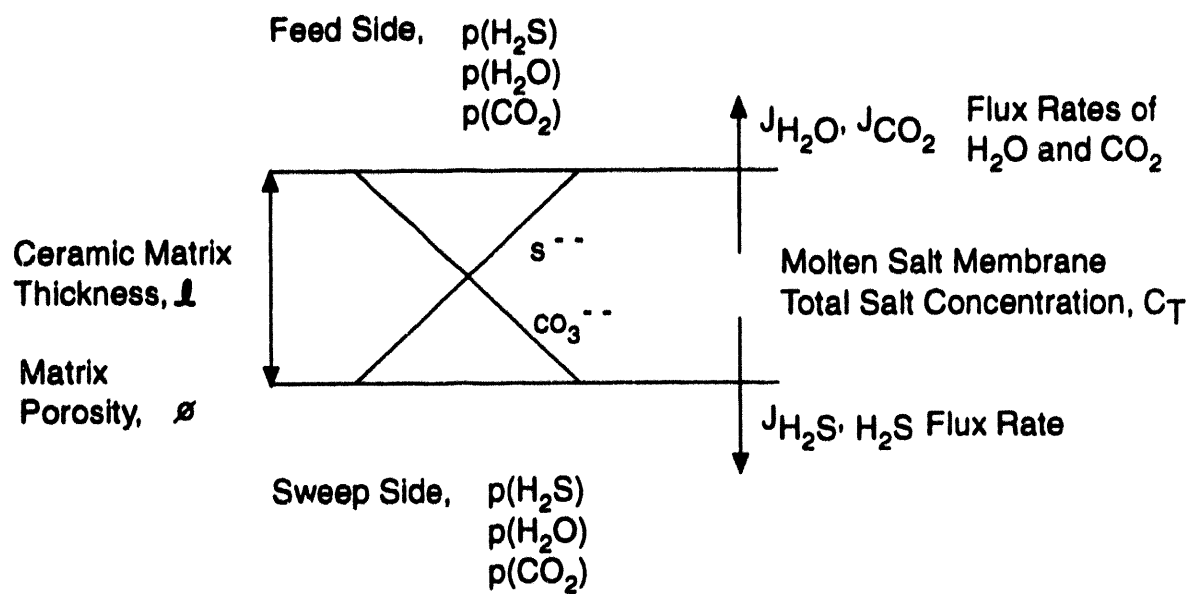


Figure 4-1. Schematic of concentration gradients in the molten salt.

where

- J_{H_2S} = Flux rate of H_2S (gmole/sec)
 $D_{S^{--}}$ = Diffusivity of S^{--} in liquid phase (cm^2/s)
 l = Membrane thickness (cm)
 A = Membrane surface area (cm^2)

substituting for X

$$J_{H_2S} = \frac{D_{S^{--}} A C_T}{l} \left[\frac{K p(H_2S)}{K p(H_2S) + p(H_2O) p(CO_2)} \Big|_{feed} - \frac{K p(H_2S)}{K p(H_2S) + p(H_2O) p(CO_2)} \Big|_{sweep} \right] \quad (4-9)$$

Since 1 mol of H_2S transport from feed side to sweep side produces transport of 1 mol of CO_2 and H_2O in the opposite direction,

$$J_{H_2O} = J_{CO_2} = J_{H_2S} \quad (4-10)$$

4.2 ESTIMATION OF K AND $D_{S^{--}}$ FROM STEADY-STATE EXPERIMENTAL PERMEATION DATA

Equation (4-9) contains two unknown parameters, K and $D_{S^{--}}$, which must be determined from the experimental data. Since the number of unknowns in the above equation is 2, steady-state H_2S permeation data are need at two different partial pressures of H_2S . As seen from Table 3-3, such data were collected in Runs No. 6 and 14.

4.2.1 Data from Run No. 6

One set of permeation data was collected using 2 percent H_2S in N_2 as feed gas at 50 psig system pressure. No steam or CO_2 were present in feed gas. Thirty percent CO_2 in N_2 was used as sweep gas with approximately 16.8 percent water vapor. The measured dry H_2S permeate concentration was 9.5 ppm with a dry sweep gas flow rate of 994 std. cm^3/min .

Thus, $p(H_2S)$ on feed side ~ 0.088 atm
 $p(H_2O)$ on sweep side ~ 0.737 atm
 $p(CO_2)$ on sweep side ~ 1.1 atm.

H_2S concentration on sweep side ~ 9.5 ppm dry
 ~ 7.9 ppm wet
 $p(H_2S)$ on sweep side ~ 3.48×10^{-5} atm.

The H₂S flux rate is ~ 7.03 x 10⁻⁹ gmol/sec. Since 1 mol of H₂S transport from feed side to sweep side results in 1 mol of CO₂ and H₂O transport, the concentrations of CO₂ and H₂O on feed side can be estimated using H₂S flux rate:

$$\begin{aligned} p(\text{H}_2\text{O}) \text{ on feed side} &\sim 3.52 \times 10^{-5} \text{ atm} \\ p(\text{CO}_2) \text{ on feed side} &\sim 3.52 \times 10^{-5} \text{ atm.} \end{aligned}$$

Substituting the above values in Equation (4-9):

$$7.03 \times 10^{-9} = \left(\frac{D_s \cdot A \cdot C_T}{l} \right) \quad (4-11)$$

$$\left[\frac{0.088 K}{0.088 K + (3.52 \times 10^{-5}) \cdot (3.52 \times 10^{-5})} - \frac{3.48 \times 10^{-5} \cdot K}{(3.48 \times 10^{-5}) \cdot K + 0.737 \times 1.1} \right]$$

In Run No. 6, another set of permeation data was collected using 0.6 percent H₂S in the feed gas. The feed gas contained 9 percent CO and 6 percent H₂; however, it did not contain any CO₂. The steam used on the test side was approximately 15.9 percent. The water gas shift reaction between H₂O and CO is likely to produce some CO₂ at the experimental temperatures. The analysis of feed exit gas indicated presence of about 0.25 percent CO₂.

$$\begin{aligned} \text{Thus, } p(\text{H}_2\text{S}) \text{ on feed side} &\sim 0.022 \text{ atm} \\ p(\text{H}_2\text{O}) \text{ on feed side} &\sim 0.7 \text{ atm} \\ p(\text{CO}_2) \text{ on feed side} &\sim 0.011 \text{ atm.} \end{aligned}$$

Thirty percent CO₂ in N₂ was again used as sweep gas with 16.8 percent steam.

$$\begin{aligned} \text{Thus, } p(\text{H}_2\text{O}) \text{ on sweep side} &\sim 0.737 \text{ atm} \\ p(\text{CO}_2) \text{ on sweep side} &\sim 1.1 \text{ atm.} \end{aligned}$$

$$\begin{aligned} \text{The H}_2\text{S concentration on sweep side} &\sim 2.8 \text{ ppm dry} \\ &\sim 2.33 \text{ ppm wet} \\ p(\text{H}_2\text{S}) \text{ on sweep side} &\sim 1.03 \times 10^{-5} \text{ atm.} \end{aligned}$$

The H₂S flux rate was ~ 2.07 x 10⁻⁹ gmol/sec. Substituting the above set of values in Equation (4-9):

$$2.07 \times 10^{-9} = \left(\frac{D_s \cdot A \cdot C_T}{l} \right) \quad (4-12)$$

$$\left[\frac{0.022 K}{0.022 K + 0.011 \times 0.7} - \frac{1.03 \times 10^{-5} \cdot K}{1.03 \times 10^{-5} \cdot K + 0.737 \times 1.1} \right]$$

Solving Equations (4-11) and (4-12):

Equilibrium constant, K ~ 0.15 atm at 560 °C, and

$$\frac{D_{S^{--}} \cdot C_T \cdot A}{l} = 7.03 \times 10^{-9} \text{ gmol/sec} .$$

For 49 percent Li_2CO_3 , 25 percent K_2CO_3 , and 26 percent CaCO_3 mixture, the liquid salt density is $\sim 2.54 \times 10^{-2} \text{ gmol/cm}^3$. The percent salt infiltration for membrane used in Run No. 6 was 68 percent. Assuming ceramic matrix porosity of 0.5 the molar salt concentration in the membrane, C_T , was $\sim 8.64 \times 10^{-3} \text{ gmol/cm}^3$. The membrane thickness was $\sim 0.25 \text{ cm}$ and the effective membrane surface area was estimated to be 2.3 cm^2 .

Thus, $D_{S^{--}} \sim 8.84 \times 10^{-8} \text{ cm}^2/\text{sec}$
 \sim Diffusivity of S^{--} in molten salt at $560 \text{ }^\circ\text{C}$.

4.2.2 Data from Run No. 14

During this run, one set of permeation data was collected using 2.9 percent H_2S in N_2 as feed gas at 50 psig system pressure. No steam or CO_2 were present in feed gas. Thirty percent CO_2 in N_2 was used as sweep gas with approximately 16.8 percent steam. The measured dry H_2S permeate concentration was 16.3 ppm with a dry sweep gas flow rate of $1,000 \text{ std. cm}^3/\text{min}$.

Thus, $p(\text{H}_2\text{S})$ on feed side = 0.13 atm
 $p(\text{H}_2\text{O})$ on sweep side = 0.737 atm
 $p(\text{CO}_2)$ on sweep side = 1.1 atm
 $p(\text{H}_2\text{S})$ on sweep side = $6 \times 10^{-5} \text{ atm}$
 H_2S flux rate = $1.21 \times 10^{-8} \text{ gmol/sec}$
 $p(\text{H}_2\text{O})$ on feed side = $7.2 \times 10^{-5} \text{ atm}$.
 $p(\text{CO}_2)$ on feed side = $7.2 \times 10^{-5} \text{ atm}$.

Substituting the above values in Equation (4-9)

$$1.21 \times 10^{-8} = \left(\frac{D_{S^{--}} A C_T}{l} \right) \left[\frac{0.13 K}{0.13 K + 7.2 \times 10^{-5} \times 7.2 \times 10^{-5}} - \frac{6 \times 10^{-5} K}{6 \times 10^{-5} + 0.737 \times 1.1} \right] . \quad (4-13)$$

Solving the above equation

$$\frac{D_{S^{--}} A C_T}{l} = 1.21 \times 10^{-8} \text{ gmol/sec} . \quad (4-14)$$

Data were also obtained at 100 and 200 psig system pressure and the same gas compositions. The corresponding H_2S permeation rates observed were 16.5 and 17.1 ppm, respectively. These steady-state values were not significantly different than those obtained at 50 psig pressure conditions. Inspection of Equation (4-13) indicates that these results are consistent, since pressure does not have a significant effect on liquid phase diffusivity.

In Run No. 14, another set of permeation data was collected using 0.6 H₂S in feed gas with 6 percent CO₂. The steam used on feed side was about 25.2 percent. Thirty percent CO₂ in N₂ was used as sweep gas with 25.9 percent water vapor. The steady-state H₂S concentrations were obtained at two system pressures of 50 and 100 psig and were 4.3 and 3.0 ppm, respectively. The dry sweep gas flow rate in both cases was 1,000 std. cm³/min.

Thus, for 50 psig system operation,

$$\begin{aligned} p(\text{H}_2\text{S}) \text{ on feed side} &= 0.021 \text{ atm} \\ p(\text{CO}_2) \text{ on feed side} &= 0.21 \text{ atm} \\ p(\text{H}_2\text{O}) \text{ on feed side} &= 1.11 \text{ atm} \\ p(\text{H}_2\text{O}) \text{ on sweep side} &= 1.14 \text{ atm} \\ p(\text{CO}_2) \text{ on sweep side} &= 1.05 \text{ atm} \\ p(\text{H}_2\text{S}) \text{ on sweep side} &= 1.5 \times 10^{-5} \text{ atm} \end{aligned}$$

$$\text{and H}_2\text{S flux rate} = 3.2 \times 10^{-9} \text{ gmol/sec.}$$

Substituting the above values in Equation (4-9), using Equation (4-12) and solving

$$K = 3.98 \text{ atm.}$$

At 100 psig system operation,

$$\begin{aligned} p(\text{H}_2\text{S}) \text{ on feed side} &= 0.037 \text{ atm} \\ p(\text{CO}_2) \text{ on feed side} &= 0.37 \text{ atm} \\ p(\text{H}_2\text{O}) \text{ on feed side} &= 1.97 \text{ atm} \\ p(\text{H}_2\text{O}) \text{ on sweep side} &= 2.02 \text{ atm} \\ p(\text{CO}_2) \text{ on sweep side} &= 1.86 \text{ atm} \\ p(\text{H}_2\text{S}) \text{ on sweep side} &= 1.86 \times 10^{-5} \text{ atm.} \end{aligned}$$

Substituting the above values in Equation (4-9), using Equation (4-12) and solving

$$K = 4.47 \text{ atm.}$$

The above value of K is close to that calculated from data collected at 50 psig pressure. Thus, these data are consistent with facilitated transport mechanism for H₂S. This value of K is, however, much higher than that obtained in Run No. 6. One important difference in these two runs was the lack of CO₂ in the feed gas used in Run No. 6. The feed side CO₂ concentration in that case was measured by a GC. Any error in that measurement can have a substantial effect in calculations. The liquid phase diffusivity, based on data in Run No. 14, is estimated to be 1.56×10^{-7} cm²/sec. This value for D_{S--} is very close to that obtained from Run No. 6 data.

4.3 ANALYSIS OF TRANSIENT DATA

Analysis of the H₂S transport process as given in Section 4-1 allows estimation of the reaction equilibrium constant and liquid phase diffusivity using steady-state permeation data. Almost all of the membrane experiments have indicated a gradual rise in H₂S concentrations with time. Referring to Figure 4-1, this time requirement may be considered as that required for development of the concentration gradients in the liquid phase.

Starting with a fresh molten salt membrane, the sulfide ion [S²⁻] concentrations would be zero initially throughout the liquid phase. As the feed side of the molten salt membrane is exposed to a gas containing H₂S, the concentration of the S²⁻ ion on the feed side surface of the membrane may be assumed to reach the equilibrium concentration instantaneously. The development of the concentration gradient in the liquid phase of the membrane may be considered to be diffusion of the S²⁻ ions within the liquid film, similar to diffusion in an infinite length slab. The diffusion of S²⁻ ions in a semi-infinite membrane of thickness l may be expressed as

$$\frac{\partial C}{\partial t} = D \frac{\partial^2 C}{\partial \chi^2} \quad (4-15)$$

where

C = concentration of S²⁻ ions in the liquid phase at time t and position χ (gmole/cm³)

t = time (sec)

D = Diffusivity of S²⁻ ions in the liquid phase (cm²/sec)

χ = Distance across a membrane from the sweep side of the membrane (cm).

The initial condition is given as

$$C(\chi, t) = 0 \text{ for } t=0 \text{ and } 0 < \chi < l.$$

Since there is no H₂S in the sweep gas, the sulfide ion concentration on the sweep side surface of the membrane may be assumed to be zero.

The sulfide ion concentration at the feed side surface of the membrane is assumed to be that given by the reaction equilibrium, C_0 , which would be constant with time for constant feed gas composition. Thus, the boundary conditions are

$$\begin{aligned} C &= 0, \text{ for } \chi = 0, t \geq 0 \text{ and} \\ C &= C_0, \text{ for } \chi = l, t \geq 0 \end{aligned}$$

The development of concentration profile with t and X is given by solution of Equation (4-13) (Crank, 1964):

$$C(\chi, t) = C_0 \frac{\chi}{l} + \frac{2}{\pi} \sum_{n=1}^{\infty} C_0 \frac{\cos(n\pi)}{n} \cdot \sin \frac{(n\pi\chi)}{l} \cdot e^{-Dn^2\pi^2 t/l^2} \quad (4-16)$$

The above solution indicates that steady state is practically achieved in dimensionless time, $\frac{Dt}{l^2}$, of 0.45. A cumulative amount of the species permeated is obtained by integrating

the above solution and is given by Crank (1964) as:

$$\frac{Q_t}{l C_0} = \frac{Dt}{l^2} - \frac{1}{6} - \frac{2}{\pi^2} \sum_{n=1}^{\infty} \frac{(-1)^n}{n^2} e^{-Dn^2\pi^2 t/l^2} \quad (4-17)$$

where Q_t is a cumulative permeated amount of the diffusing species (gmole/cm²). The flux rate at any given time is obtained by differentiating Q_t with time in Equation (4-15)

$$\frac{d \left[\frac{Q_t}{l C_0} \right]}{dt} = \frac{D}{l^2} + \frac{2D}{l^2} \sum_{n=1}^{\infty} (-1)^n e^{-\frac{Dn^2\pi^2 t}{l^2}} \quad (4-18)$$

or

$$\frac{\frac{dQ_t}{dt}}{\left[\frac{DC_0}{l} \right]} = \frac{(\text{Flux})_t}{(\text{Flux})_{\text{maximum}}} = 1 + 2 \sum_{n=1}^{\infty} (-1)^n e^{-n^2\pi^2 \left[\frac{Dt}{l^2} \right]} \quad (4-19)$$

The right side of the above equation was evaluated numerically for different values of dimensionless time, $\frac{Dt}{l^2}$, and is plotted in Figure 4-2. The H₂S flux rate through the molten

salt membrane is directly proportional to the measured H₂S concentration in the sweep outlet gas. Thus, Figure 4-2 simulates a gradual increase in permeate H₂S concentration with time. This figure may be compared with the observed gradual increase in H₂S concentration to determine the diffusion coefficient of S²⁻ ions in the liquid phase. For example, the initial transient data obtained with fresh membrane in Runs No. 6, 8, and 14 as seen in Figures 3-1, 3-4, and 3-6 may be used to estimate the diffusion coefficient.

4.3.1 Estimates of Diffusion Coefficient from Experimental Data

As seen in Figure 3-4, the time required to reach the peak H₂S concentration in Run No. 8 was about 800 min, although H₂S concentration actually stabilized after about 1,300 min. In Run No. 14, also the time required to reach steady state at 50 psi conditions was found to be about 1,300 min. Since the dimensionless time needed to achieve a practical steady state is about 0.45 and the membrane thickness is about 0.25 cm, the liquid phase diffusivity is estimated to be

$$D \sim \frac{0.45 \cdot l^2}{t} \sim \frac{0.45 \times 0.25 \times 0.25}{1,300 \times 60} \quad (4-20)$$

$$\sim 3.6 \times 10^{-7} \text{ cm}^2/\text{sec}$$

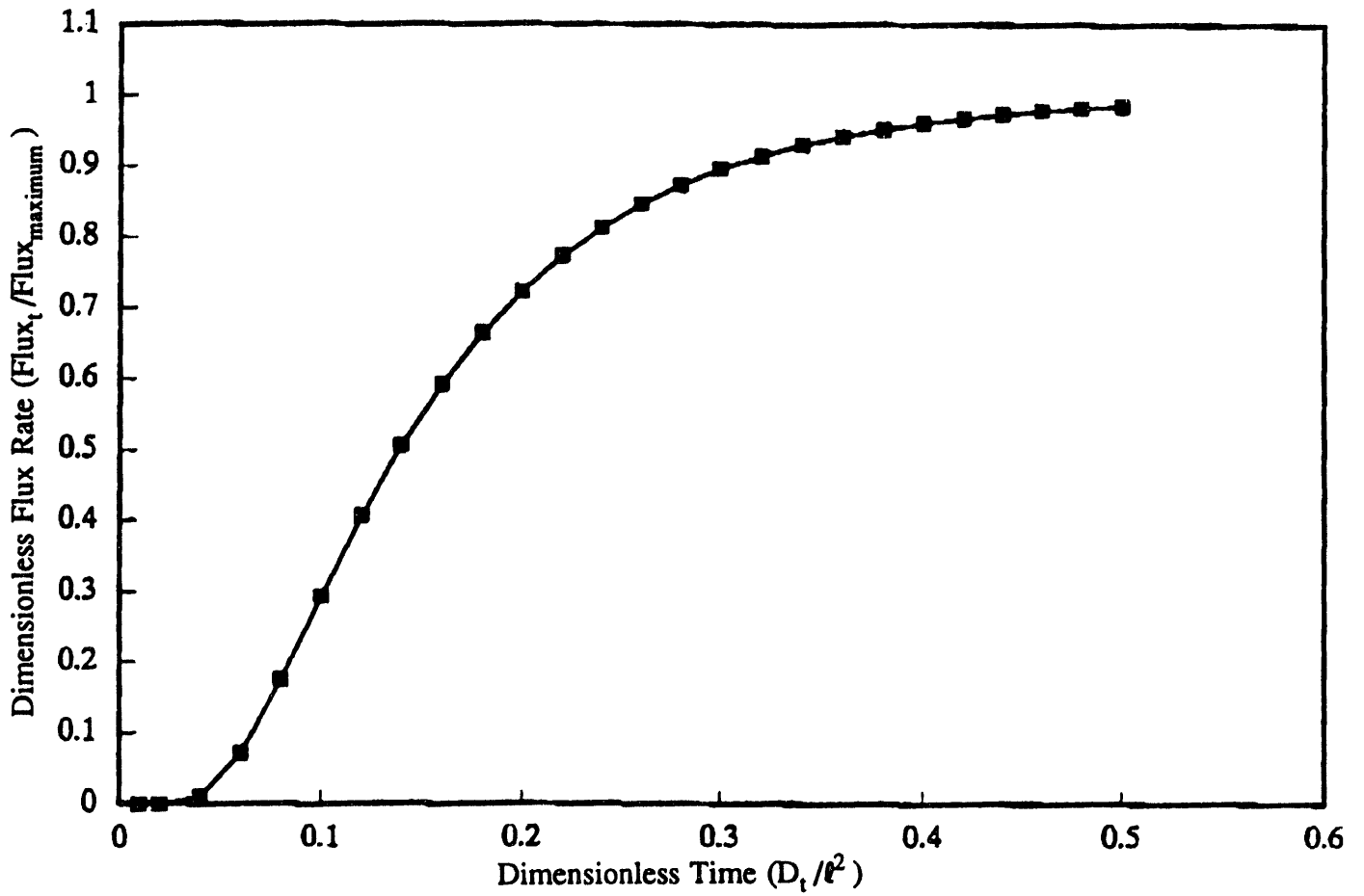


Figure 4-2. Variation of flux rate with time—diffusion through a plane sheet.

From Figure 4-2 it can be seen that a more reliable estimate of diffusivity may be obtained by comparing time required to reach 50 percent of the steady-state level, since this point would be in the zone of steeper rise in concentrations. From Figure 4-2, a dimensionless time of 0.15 would be needed to reach 50 percent of the steady-state concentration level. In Run No. 6 the steady-state H₂S concentration with coal gas at 50 psig condition was about 2.5 ppm. From Figure 3-1, the time required to reach half of this level was about 300 min. In Figure 3-4 the time required to reach half of the peak H₂S concentration of 6 ppm in Run No. 8 was about 600 min, whereas half of the ultimate steady-state concentration of 2.5 ppm was reached in about 400 min. In Run No. 14 the time required to reach half of the peak concentration was much longer, on the order of 1,000 min. The theoretical analysis assumes that the H₂S reaction with salt and diffusion of S⁻ ions in liquid phase is the only possible mechanism for H₂S transport. Whereas, in actual cases, porous viscous and diffusive flow contributed significantly to the overall H₂S transport, thus contributing to the observed variability in the times required to reach half of the apparent steady-state levels. Also, it is interesting to note that the onset time required for first measurable H₂S detection was also significantly different in all three runs ranging from 180 min to 500 min. As discussed in Section 3.2.10, the observed nonuniformities in salt infiltration in the membranes can substantially affect the permeation characteristics. The time required to reach half of the apparent steady-state varied from 300 to 1,000 min. The corresponding calculated diffusivity values range from 5x10⁻⁷ to 2x10⁻⁷ cm²/sec. The value of liquid phase [S⁻] diffusion coefficient based upon transient analysis (2 to 5x10⁻⁷ cm²/sec) compares fairly well with 8.8x10⁻⁸ cm²/sec calculated from one set of steady-state permeation data.

4.4 MAXIMUM ACHIEVABLE H₂S CONCENTRATION IN PERMEATE

One of the requirements for a successful application of a facilitated transport membrane is its ability to transport H₂S in uphill direction against the H₂S concentration gradient across a membrane. The membrane permeation data collected in tests with disc membranes thus far indicate substantial diffusional resistance in the present membrane configuration. Theoretical analysis was therefore conducted to determine the maximum achievable H₂S concentration in the sweep gas in a hypothetical case of no diffusional resistance. In such a case, the H₂S concentration in the permeate would be dictated solely by the reaction equilibrium. The data collected in Run No. 6, indicated an equilibrium constant for H₂S-carbonate salt reaction of about 0.15 atm. This equilibrium constant may be used to determine the maximum possible H₂S transport across a membrane for a given set of operating conditions.

The equilibrium constant, which is estimated to be 0.15 atm, based on Run No. 6, is expressed as

$$\frac{[S^-] [H_2O] [CO_2]}{[CO_3^{--}] [H_2S]} = 0.15 \quad (4-21)$$

where [S⁻] and [CO₃⁻⁻] are ionic concentrations in the molten salt (gmole/cm³) and [H₂O], [CO₂], and [H₂S] are the partial pressures, atmospheres, of the respective species in the gas phase in contact with the molten salt surface. This equilibrium constant would be applicable to both the feed and permeate sides of the membrane. Within the liquid phase molten salt, the S⁻ and CO₃⁻⁻ ions migrate according to the concentration gradient for the respective ionic species. Therefore, the criterion for H₂S transport across the molten salt membrane is that there should be a positive gradient for [S⁻] ions from the feed side to the permeate side of a membrane. For a KRW

gasifier, the coal gas typically consists of 0.5 percent H₂S, 5 percent CO₂, and 15 percent steam. Thus, for a pressure of P atmospheres on the feed side, the ratio of S²⁻ and CO₃²⁻ concentrations on the feed side of the membrane is given by

$$\frac{[S^{2-}]}{[CO_3^{2-}]} = \frac{0.15 \cdot P \cdot \frac{0.5}{100}}{P \cdot \frac{15}{100} \cdot P \cdot \frac{5}{100}} \quad (4-22)$$

$$\frac{[S^{2-}]}{[CO_3^{2-}]} = \frac{0.1}{P_{\text{feed}}} \text{ or } \frac{0.2 \cdot (X_{H_2S})_{\text{feed}}}{P_{\text{feed}}}$$

where $(X_{H_2S})_{\text{feed}}$ is the percent of H₂S on the feed side gas.

On the sweep side the maximum CO₂ and H₂O concentrations would be 50 percent with no H₂S in the sweep gas, 49 percent with 2 percent H₂S in the sweep gas and $(100 - X_{H_2S}/2)$ where, X_{H_2S} is the sweep (permeate) gas percent H₂S.

Thus, for a pressure of P_{sweep} atmospheres on the sweep side, the ratio of the ionic concentrations of S²⁻ and CO₃²⁻ in the molten salt on the permeate side of the surface is given by

$$\frac{[S^{2-}]}{[CO_3^{2-}]} \Big|_{\text{sweep}} = \frac{0.15 \cdot 400 \cdot X_{H_2S}}{(100 - X_{H_2S}) \cdot (100 - X_{H_2S}) \cdot P_{\text{sweep}}} \quad (4-23)$$

For positive S²⁻ gradient from the feed side to the permeate side across the membrane:

$$\frac{[S^{2-}]}{[CO_3^{2-}]} \Big|_{\text{feed}} > \frac{[S^{2-}]}{[CO_3^{2-}]} \Big|_{\text{sweep}} \quad (4-24)$$

$$\frac{0.1}{P_{\text{feed}}} > \frac{60}{P_{\text{sweep}}} \frac{X_{H_2S}}{(100 - X_{H_2S})^2}$$

For maximum permeate X_{H_2S}

$$\frac{0.1}{P_{\text{feed}}} = \frac{60}{P_{\text{sweep}}} \frac{X_{H_2S}}{(100 - X_{H_2S})^2} \quad (4-25)$$

Thus, for a pressure ratio of $[P_{\text{feed}} / P_{\text{sweep}}]$ equal to one, the maximum H_2S concentration on the permeate sweep side would be 12.75 percent. With a feed pressure to sweep pressure ratio of 3, the maximum possible H_2S concentration in the permeate would be limited to 5 percent, whereas with a sweep pressure to feed pressure ratio of 3, up to 27 percent H_2S concentration in the permeate could be possible. This apparently anomalous behavior is a result of the coupled transport of H_2O and CO_2 in the molten salt in the opposite direction of the H_2S transport.

SECTION 5

PROCESS EVALUATION

The data collected in long-term disc and tubular membrane experiments indicated permeability of molten salt impregnated ceramic membranes for H₂S of 10,000 to 200,000 Barrers. The maximum membrane selectivity for H₂S with respect to helium was about 18. The membranes tested exhibited substantial permeation for both helium and hydrogen, with helium permeabilities ranging from 10,000 to 40,000 Barrers. Such a large permeability for an inert gas like helium indicates substantial porous leakage flow across the molten salt membranes.

The tubular membranes exhibited substantial movement of the molten salt within the membrane at temperatures of 530 °C or higher which is only 30 °C above the salt melting point. The downward flow of salt was also observed in the long-term disc membrane experiments. These observations indicate that the porous aluminum nitride matrix is unable to hold salt in pores by capillary action due to presence of large pores. Calculations indicate that 1 μm pores should be able to hold salt in place by capillary action at up to 70 psi pressure differentials across the membrane. Thus pores considerably greater than 1 μm may be present in the ceramic matrix.

For practical application of the facilitated transport membranes in coal gas environment, the membranes must be able to concentrate the H₂S permeated to sweep side. The process analysis presented in Section 4.4 suggested that with no pressure differential across the membrane, i.e., $[P_{\text{feed}}/P_{\text{sweep}}]$ equal to one, it would be possible to concentrate H₂S from 0.6 percent H₂S coal gas on feed side to almost 13 percent (or by a factor of 20) on the permeate side. The H₂S concentration in the sweep gas can be increased even more by increasing sweep side pressure. With a sweep pressure to feed pressure ratio of 3, H₂S can be concentrated to 27 percent in the permeate. These theoretical calculations obviously indicate that this concept is promising.

Above theoretical analysis of the membrane process assumed an instantaneous establishment of the liquid phase concentration gradients. The membrane experiments with 0.25-cm thick disks indicated that up to 1300 minutes may be needed to achieve steady state permeation. For tubular membranes the time needed to achieve steady state appears to be even longer with 0.35-cm thickness membrane tubes.

For practical applications of molten salt impregnated ceramic membranes the time needed to achieve a steady-state operation needs to be much shorter, i.e., <1 hour. From the analysis of a transient diffusion process presented in Section 4.3, the time required to achieve steady state is inversely proportional to the liquid phase diffusion coefficient and is directly proportional to the square of the membrane thickness. Liquid phase diffusion coefficient is a function of temperature which cannot be changed significantly for the molten salt membrane operations. Thus, for faster steady-state operation within <1 hour, the membrane thickness needs to be reduced by an order of magnitude.

5.1 ESTIMATION OF MEMBRANE MODULE SIZE FOR A 100-MW IGCC PLANT

For a 100-MW IGCC plant using a KRW gasifier the approximate coal feed gas composition would consist of 10 percent H₂, 15 percent CO, 5 percent CO₂, 15 percent H₂O, 0.5 percent H₂S, 0.3 percent NH₃ with balance of N₂. For a pressurized gasifier like the KRW gasifier, the pressure is typically 25 atm and temperature is 600 °C. The approximate gas flow rate at 25 atm and 600 °C is estimated to be 6.7x10⁵ ft³/h. To reduce the H₂S content of the feed gas from 5,000 ppmv to 100 ppmv the amount of H₂S that needs to be removed would be

$$\begin{aligned} \text{H}_2\text{S} \\ \text{Removal} \\ \text{Rate} &= \frac{6.7 \times 10^5 \cdot (5 \times 10^{-3} - 1 \times 10^{-4}) \cdot 25 \cdot 273}{(600 + 273) \cdot 359} \\ &= 71.5 \text{ lb mol/h} . \end{aligned}$$

The observed H₂S flux rates with long-term disc membranes conducted with 0.5 percent coal gas as feed gas were of the order of 2 to 3x10⁻⁹ gmole/sec, as shown in Section 4.2. Although the disc membranes were approximately 1 in. in dia, the effective surface area exposed to feed gas was estimated to be about 2.3 cm². Thus, the observed H₂S flux rates at 50 psig and 560 °C membrane conditions with coal feed gas were about 1.1x10⁻⁹ gmol/cm²/sec or about 8x10⁻⁶ lb mol/ft²/h. Assuming that the same flux rate is observed at 25 atm and 600 °C conditions, the membrane surface area needed to remove the required 71.5 lb mol/h of H₂S is estimated to be 9x10⁶ ft².

An existing Coors Ceramics membrane unit used for filtration can pack a membrane surface area to volume of 870 ft²/ft³. With this packing density, about 10,000 ft³ of membrane volume would be needed to provide the required surface area. Nine vessels, each 10 ft in diameter and 15 ft long, would thus be needed to provide the required membrane surface area to remove 98 percent H₂S from coal feed gas for 100-MW IGCC plant.

The H₂S flux rate by facilitated transport is expected to be inversely proportional to the membrane thickness. Thus, by reducing the membrane thickness by an order of magnitude would reduce the module volume requirement to 1,000 ft³, in addition to reducing the time required for steady operation within practical limits.

The membrane operational data collected in this experimental program are of preliminary nature. The experiments also identified several practical problems such as salt movement within porous matrix and extremely long time requirement for steady-state operation. Further improvements are therefore needed for such membranes to become practical. No detailed process evaluation as well as meaningful economic evaluation can therefore be carried out at this time.

SECTION 6

CONCLUSIONS AND RECOMMENDATIONS

Molten salt impregnated ceramic disc and tubular membranes were successfully tested during this experimental program to determine their permeation characteristics for H₂S and other gases such as hydrogen. The following conclusions and recommendations can be made based on the experimental results:

- Enhanced H₂S transport with membrane selectiveness with respect to H₂S greater than unity was observed in both disc and tubular membrane studies.
- The membranes also exhibited high permeabilities for other gases, hydrogen and helium, in much excess of those expected from solution diffusion mechanism, indicating substantial porous leakage flow.
- Limited data collected at different pressures with otherwise similar conditions indicated lower H₂S permeabilities at higher pressures consistent with facilitated transport mechanism for H₂S.
- Increasing temperature produced greater H₂S permeabilities consistent with increased diffusion rate.
- Both disc and tubular membranes were successfully tested in long-term, continuous, unattended operations indicating successful experimental procedures.
- Observed membrane selectivity for H₂S with respect to helium ranged from 0.6 to 18 with bulk of values >1. The membrane selectivities for H₂S with respect to hydrogen were about half of those observed with respect to helium.
- Permeabilities of disc membranes for H₂S ranged from 13,000 to 200,000 Barrers. H₂S permeabilities of tubular membranes were substantially lower and ranged from 200 to 28,000 Barrers.
- A gradual increase in H₂S concentration was observed in most of the experiments. Such gradual increase is consistent with reaction pathway and facilitated transport mechanism for H₂S.
- The time required to achieve steady-state operation was of the order of several hours (~ 1,000 min) in the case of disc membrane experiments. For tubular membranes, steady-state operation was not observed even after several days.
- The molten salt was found to be highly mobile within the ceramic matrix at temperatures over 530 °C. This fact was readily evident in tubular membrane experiments due to rapid increase in helium and hydrogen concentration with time. Oozing of molten salt was also observed during disc membrane experiments. These observations indicate that the ceramic matrix pores were unable to hold salt by capillary suction.

- The performance of disc membranes was found to be inconsistent with a large variation in observed permeabilities. Inspection of cross section of these membranes indicated nonuniform and/or incomplete infiltration of salt within the matrix.
- For practical application of the molten salt impregnated ceramic membranes the observed H₂S flux rates need to be increased by an order of magnitude and the time requirement to achieve steady-state operation needs to be reduced by two orders of magnitude.
- The mean pore size of the ceramic matrix needs to be reduced with elimination of presence of large pores (>1 μm) to improve retention of molten salt in the ceramic matrix.

SECTION 7

REFERENCES

- Crank, J. 1964. *Mathematics of Diffusion*, Oxford U. Press, London, p. 47-48.
- Lyke, S.E. et al. 1985a. Development of a Hot Gas Cleanup System for Integrated Coal Gasification/Molten Carbonate Fuel Cell Power Plants. Final Report DOE/MC/19077-1830.
- Lyke, S.E., et al. 1985b. Prepr. Pap., *Am. Chem. Soc., Div. Fuel Chem*, 30(4):26-35.
- Moore, R.H., et al. 1980 Molten Salt Scrubbing Process for Removal of Particles and Sulfur Compounds from Low Btu Fuel Gases. BNWL-SA-6030, Pacific Northwest Lab., Richland, WA.
- Stegen, G.E., et al. 1982. Development of a Solid Absorption Process for Removal of Sulfur from Fuel Gas. DOE/ET/11028-9.

7.4 Golden Technologies Final report

Air Products & Chemicals Inc.

Facilitate Transport Ceramic Membranes for High Temperature Gas Clean-up

Final Report

Program Goal:

The goal of this project is to demonstrate the feasibility of developing high-temperature, high-pressure facilitated transport gas separation ceramic membranes in order to control gaseous contaminants in integrated Gasification Combined Cycle (IGCC) systems. These membranes will selectively and effectively remove hydrogen sulfide (H₂S) from hot gas streams in the hostile process environment encountered in IGCC systems, at temperatures ranging from 1,000°F to 1600°F, and pressures between 200 and 700 psig.

The gaseous components to be tested shall include, at a minimum, hydrogen, carbon dioxide, carbon monoxide, hydrogen sulfide, ammonia, methane, nitrogen, carbonyl sulfide, and water.

Program Objectives

- Provide Air Products & Chemicals Inc. with a porous substrate of a defined composition as determined by their molten salt infiltration requirements.
- Prepare parts from Aluminum Nitride and Lithium Aluminate, that have a pore size of 0.3μ - 0.5μ and a porosity of 30%.
- Demonstrate repeatability of ceramic process and configuration capabilities

Statement of Work - Tasks:

<u>TASK DESCRIPTION</u>	<u>STATUS</u>
<p><u>Task 1.0: Test Plan Preparation</u></p> <p>Prepare a test plan to develop and evaluate facilitated transport ceramic membranes for reducing representative gas compositions.</p>	<p>Completed</p> <p>Attached</p>
<p><u>Task 2.2: Ceramic Membrane Substrate and Metal Seal Development</u></p> <p>Based on information and recommendations from Air Products, fabricate a ceramic membrane substrate, support system, and metal seal system capable of withstanding the high temperature and pressure requirements in Integrated Gasification Combined Cycle systems.</p>	<p>Completed</p> <p>Delivered systems and samples to APCI</p>
<p><u>Task 2.3: Membrane Fabrication and Conceptual Testing</u></p> <p>Fabricate Disc Membranes for testing using the membrane materials selected in Tasks 2.1 & 2.2. Parts will be tested at Air Products.</p>	<p>Completed</p> <p>Delivered to APCI</p>
<p><u>Task 3.1: Preparation of High Temperature, High Pressure Test Plan</u></p> <p>Assist Air Products & Chemicals Inc. in developing a test plan to demonstrate the feasibility of the molten salt membrane concepts developed in Task 2.</p>	<p>Completed</p>
<p><u>Task 3.2: Fabrication of H₂S Membrane</u></p> <p>Fabricate a series of molten salt membrane samples as identified in the test plan (Task 3.1).</p>	<p>Completed</p> <p>Delivered to APCI</p>

Project Highlights:

- Both flat discs of varying thicknesses and single bore tubes were prepared from Aluminum Nitride as requested by Air Products & Chemicals Inc.
- Tests showed that both pore diameter and porosity were controllable by specific firing profiles.
- A suitable Lithium Aluminate (LiAlO₂) raw material powder could not be found to yield the pore size and porosity required. Available powder was found with a particle size that gave pore size of 1 to 3 μ . Wet Grinding produced the correct particle size to yield the 0.5 μ pore size in the fired structure, but caused a shift to LiAl₅O₈. Dry grinding did not change the particle size to the required diameter, although the composition remained LiAlO₂.

Discussion of the Project:

Based on the literature reviews and initial test & conceptual test plans, we were requested to produce membranes of varying thicknesses out of two key materials: Aluminum Nitride, and Lithium Aluminate. Due to the pore and particle size requirements for suitable membranes, Lithium Aluminate powder of sufficiently fine particle size was *not* commercially available. Attempts to mill available raw Lithium Aluminate powders to appropriate particle sizes remains a technical difficulty as discussed below.

The Aluminum Nitride that was used for parts is a commercial available product from Dow Chemical. It was used for both the dry and iso-pressing of parts. We were unable to get discs to a thickness of 0.025" as requested without secondary forming processes. Discs at 0.100" and 0.050" thickness could be pressed and directly fired without additional forming. Best results for firing were found to be on setter covered with Boron Nitride powder. It is necessary to fire these parts in a Nitrogen Atmosphere. We found no limit to part size or configuration with the samples. When additional forming is necessary, either green forming and/or finish grinding can be performed. The most effective finish grinding method involves using a double face lab grinder to avoid "cupping" of very thin components.

The Lithium Aluminate powder was purchased from FMC corporation, Cypress Goote Mineral Co., and Johnson Mathey Catalog Co. The particle size of all these powders proved to be too large to yield the 0.5 μ pore size upon firing. Tests using both wet and dry grinding were used to reduce the particles size of raw materials to achieve the correct pore size upon firing. A wet grind of 24 hours did yield the particles size desired, but the material was contaminated by the high alumina mill and grinding media. This contamination changed the material from LiAlO₂ to LiAl₅O₈. The resultant LiAl₅O₈ changed the wetting angle of the molten salt which impeded the salt infiltration. Work was discontinued on the Lithium Aluminate material and re-focused on Aluminum Nitride.

The following tables illustrate the relationship between raw material surface area, firing temperature, and yielded porosity and pore size:

Aluminum Nitride

Firing Temperature	% Porosity	Pore Size
1550	48	0.38 μ
1600	47	0.39 μ
1650	46	0.42 μ

Lithium Aluminate (LiAlO₂)

Firing Temperature	% Porosity	Pore Size
1350	48	4.2μ
1400	50	4.0μ

Surface Area Affects on Lithium Aluminate (LiAlO₂)

Surface Area	% Porosity Fired at 1350°C	Pore Size
0.69 M ² /gm	46	4μ
① 1.40 M ² /gm	44	2.8μ
② 2.10 M ² /gm	40	2.0μ
* 4.00 M ² /gm	38	1.2μ
* 5.60 M ² /gm	38	0.7μ

① *High Intensity dry grind 4 hours*

② *High Intensity dry grind 8 hours*

* *These were achieved by wet grinding. However, it caused the chemical to change from LiAlO₂ to LiAl₅O₈ due to the ball/mill wear from 48 hour grind time.*

The resulting microstructures and performance graphs are attached.

Final Analysis & Cost of Aluminum Nitride Parts:

- Discs 0.100" thick x 1.00" in diameter \$2.00 Each
- Tubes 0.500" diameter x 6" long x 0.100" wall \$4.00 Each

From a final cost, manufacturability, and ease of handling perspective, the best thickness membrane to perform this level of separation seems to be either the 0.100" to 0.075" thicknesses. The thinner level membranes offer relatively little performance improvement at a significantly high manufacturing cost, and are more fragile to handle.

TASK 2.2 -- CERAMIC AND SEAL DEVELOPMENT -- FY 91/92 -- CONCEPT EVALUATION, DEVELOPMENT AND TESTING -- COORS CERAMICS

TASK	APRIL		MAY				JUNE
	21	28	05	12	19	26	02
I. ALUMINUM NITRIDE DEVELOPMENT							
1. RECEIVE INPUT FROM APCI	**						
2. DETERMINE TEST MATRIX	***						
3. PREPARE AlN SPECIMENS	*****						
4. CHARACTERIZE GREEN AlN	*****		*****				
5. DETERMINE FIRING SCHEDULES			*****				
6. INITIAL FIRING (HP/MOLY)			*****				
7. CHARACTERIZE FIRED AlN			*****				
8. PERFORM ADDITIONAL FIRINGS			*****				
9. CHARACTERIZE ALL FIRINGS			*****				
10. DETERMINE VARIABLE RELATIONS			*****				*****
11. Hg POROSIMETRY EVALUATIONS			*****				*****
12. SAMPLES TO APCI						*****	*****
13. POROUS DEVELOPMENT							
14. CONTROLLED POROSITY EXP'TS							
15. POROUS SAMPLES TO APCI							
16. MONTHLY PROGRESS REPORT			**				**
17. ALUMINUM TITANATE TO APCI	**						
18. MEETING IN CINCINNATI		**					

168

APCI MEMBRANE DEVELOPMENT

ID	Name	April	May	June	July	August	September	October	November	December	J	
1	LITHIUM ALUMINATE											
2	milling experiment											
3	apci replication											
4	process study											
5	initial samples											
6	membrane production											
7	ALUMINUM NITRIDE											
8	1600/10ksi samples											
9	coarse material											
10	bi-layer material											
11	MEETING AT COORS											
12	REPORTS											

Project: APCI MEMBRANE
Date: 4/10/92

Critical Noncritical

Progress Milestone Summary

APCI/COORS SHORT TERM WORK PLAN

10/04/91

OCTOBER
1991

NOVEMBER
1991

DECEMBER
1991

TASK

AIN MEMBRANES

XXXXXXXXXXXXXXXXXX

XXXXXXXXXXXXX

LIPID REPRO/MEM

XXXXXXXXXXXXXXXXXX

XXXXXXXXXXXXXXXXXXXXX

XXXXXXXXXXXXXXXXXXXXX

COARSE AIN

XXXXXXXXXXXXXXXXXX

XXXXXXXXXXXXXXXXXXXXX

XXXXXX

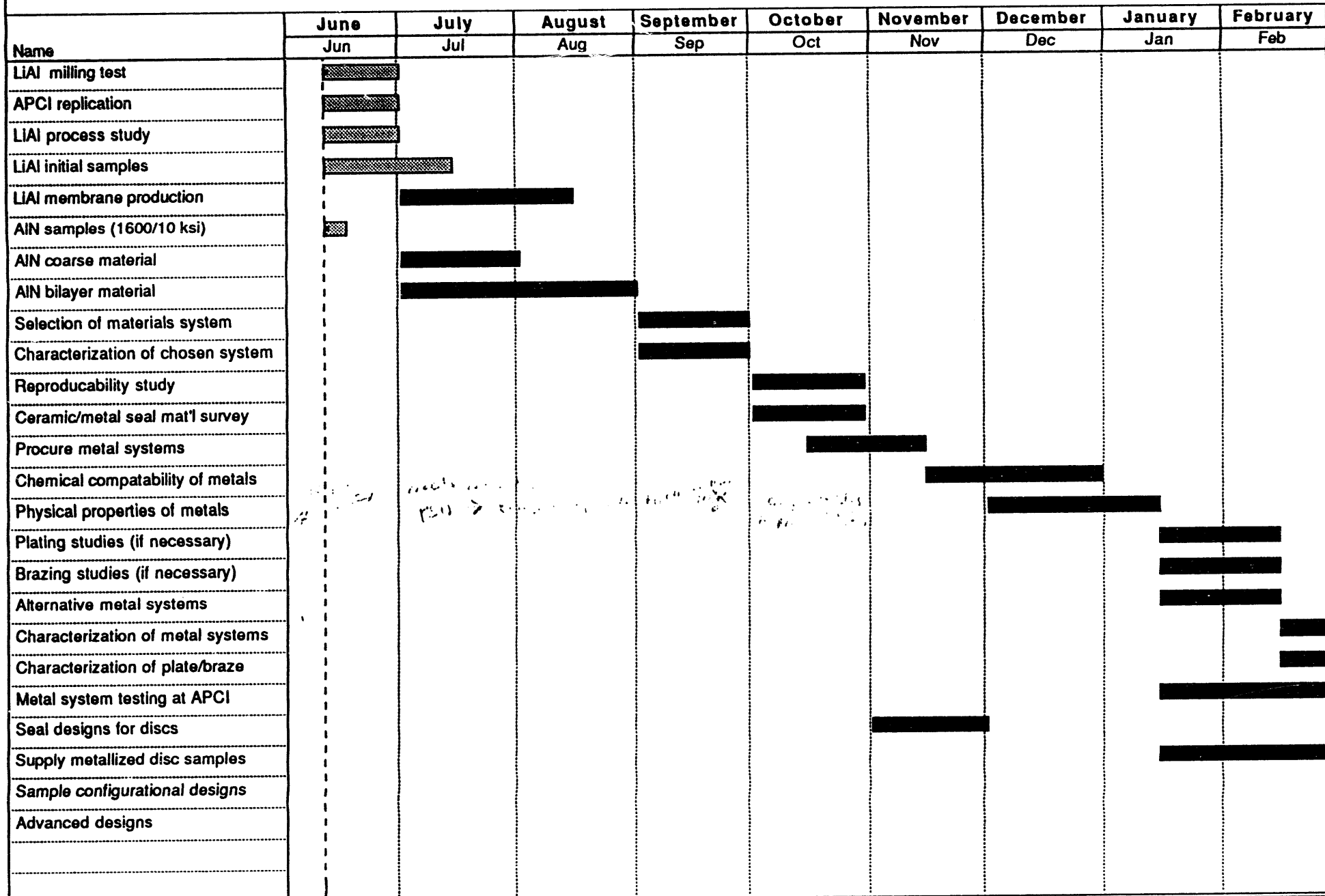
BILAYER AIN

XXXXXXXXXXXXXXXXXXXXX

AIN/BN HYBRIDS

XXXXXX

APCI FACILITATED TRANSPORT CONTRACT -- 1992-93



171

Project: APCI CONTRACT 92-93
Date: 6/11/92

Critical Progress Summary
 Noncritical Milestone

APCI FACILITATED TRANSPORT CONTRACT - 1992-93

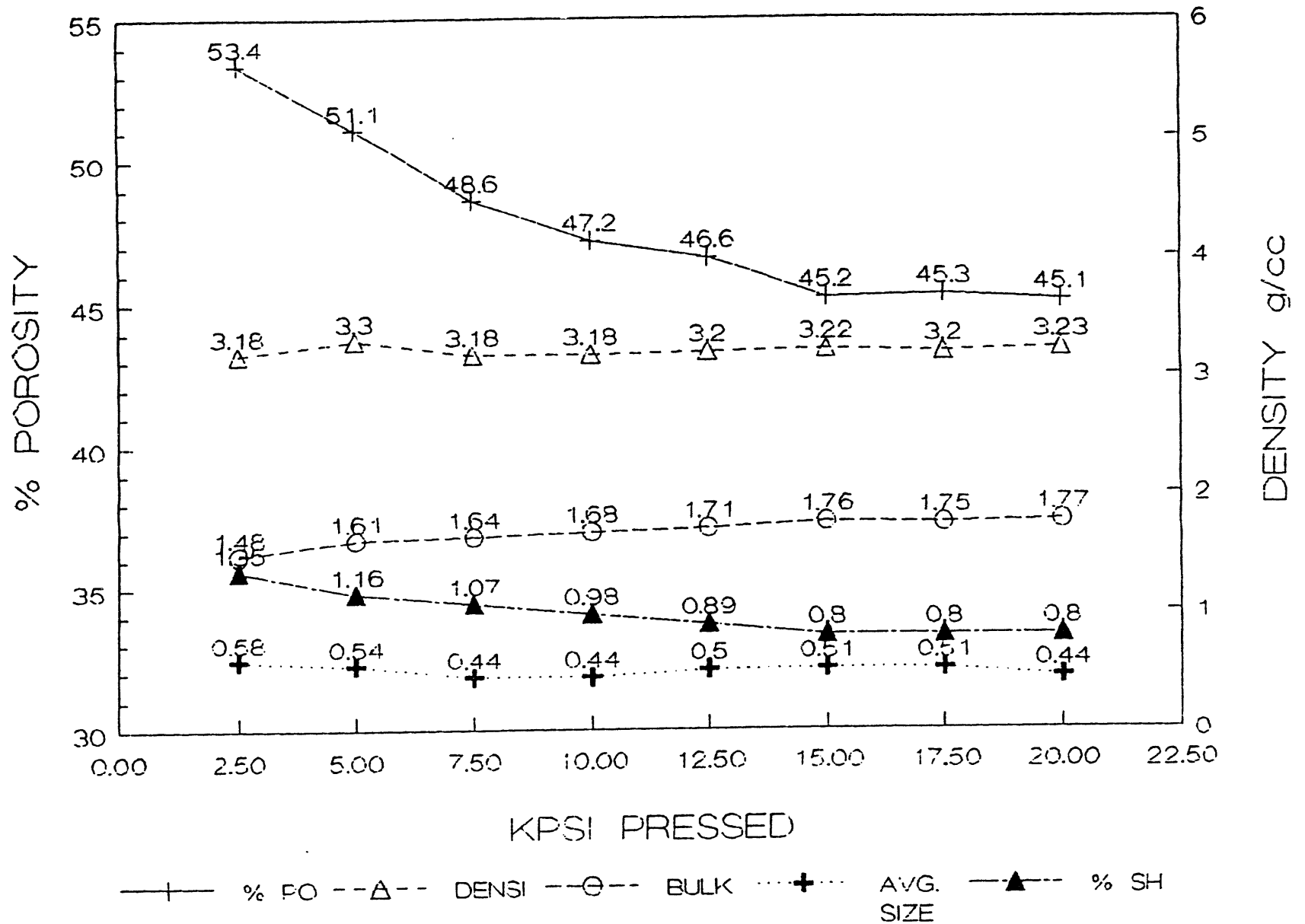
March Mar	April Apr	May May	June Jun	July Jul	August Aug	September Sep	October Oct	November Nov	December Dec	January Jan

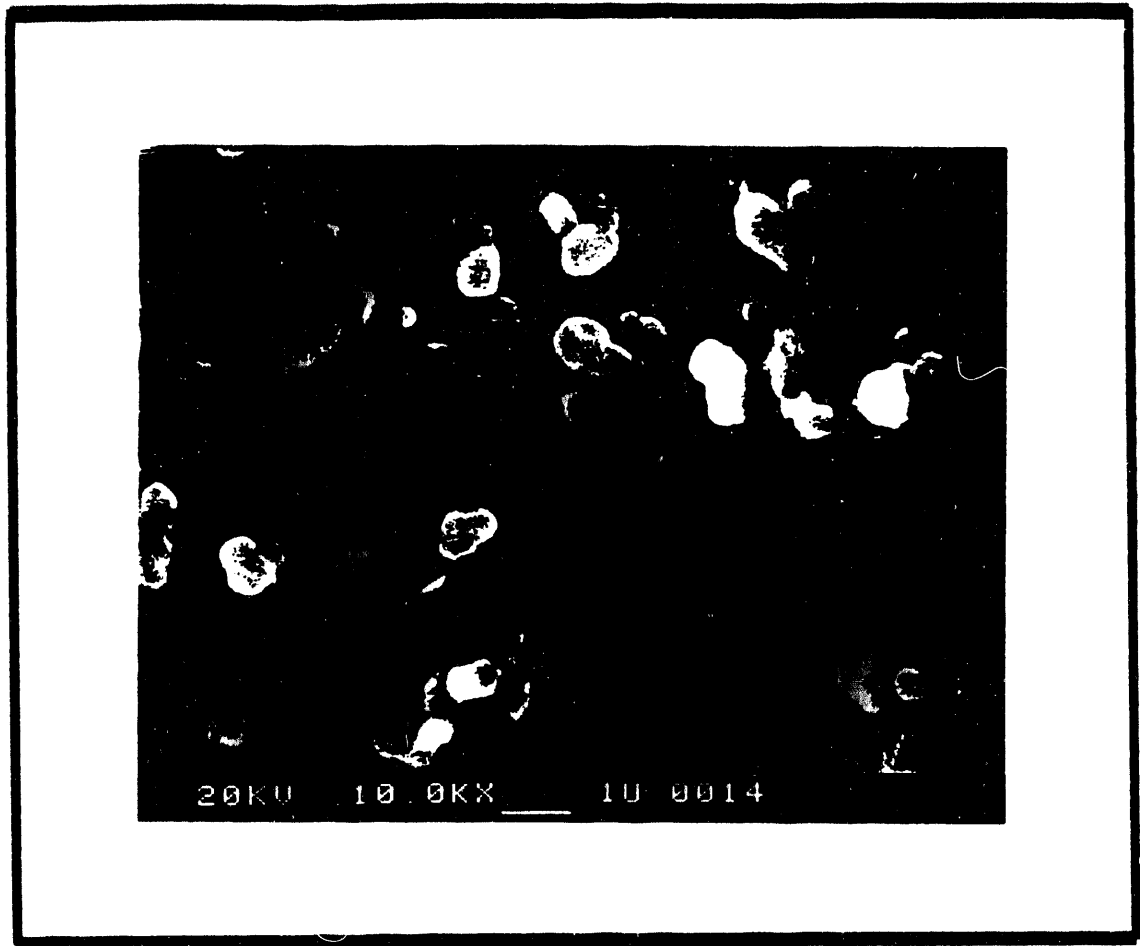
Project: APCI CONTRACT 92-93
Date: 6/11/92

Critical  Progress  Summary 
 Noncritical  Milestone 

AIN DELTECH FIRING 1600 C/1 HR

173





POROUS ALUMINUM NITRIDE

FIRING: 1600 C, DELTECH/CRUCIBLE

LOT #: 71

PRESSURE: 10 KPSI

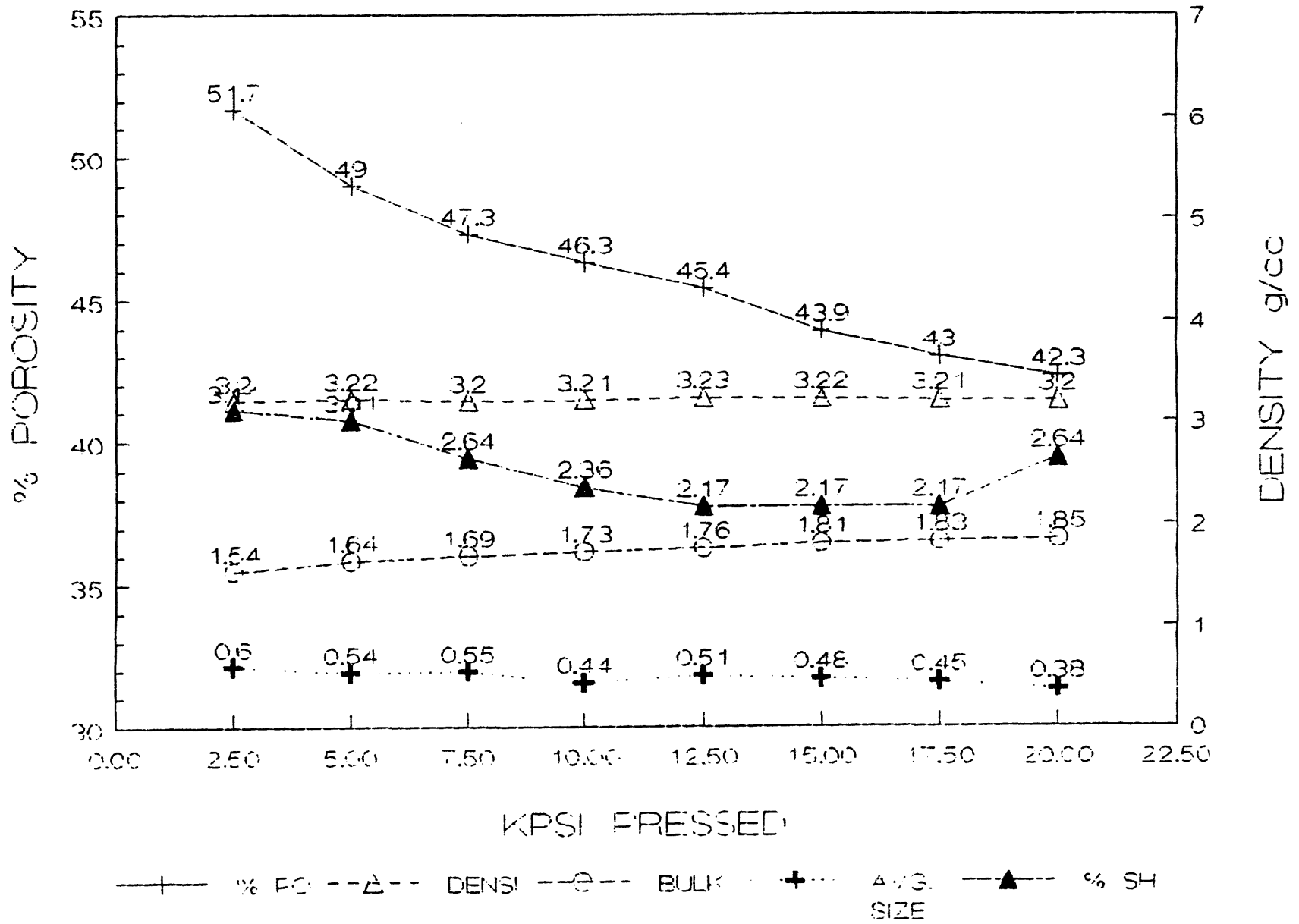
MAGNIFICATION: 10,000 X

SAMPLE PREP: FRACTURE SURFACE

DATE: 06/01/91

AIN DELTECH FIRING 1650 C/1 HR

175





POROUS ALUMINUM NITRIDE

FIRING: 1650 C, DELTECH/CRUCIBLE

LOT #: 71

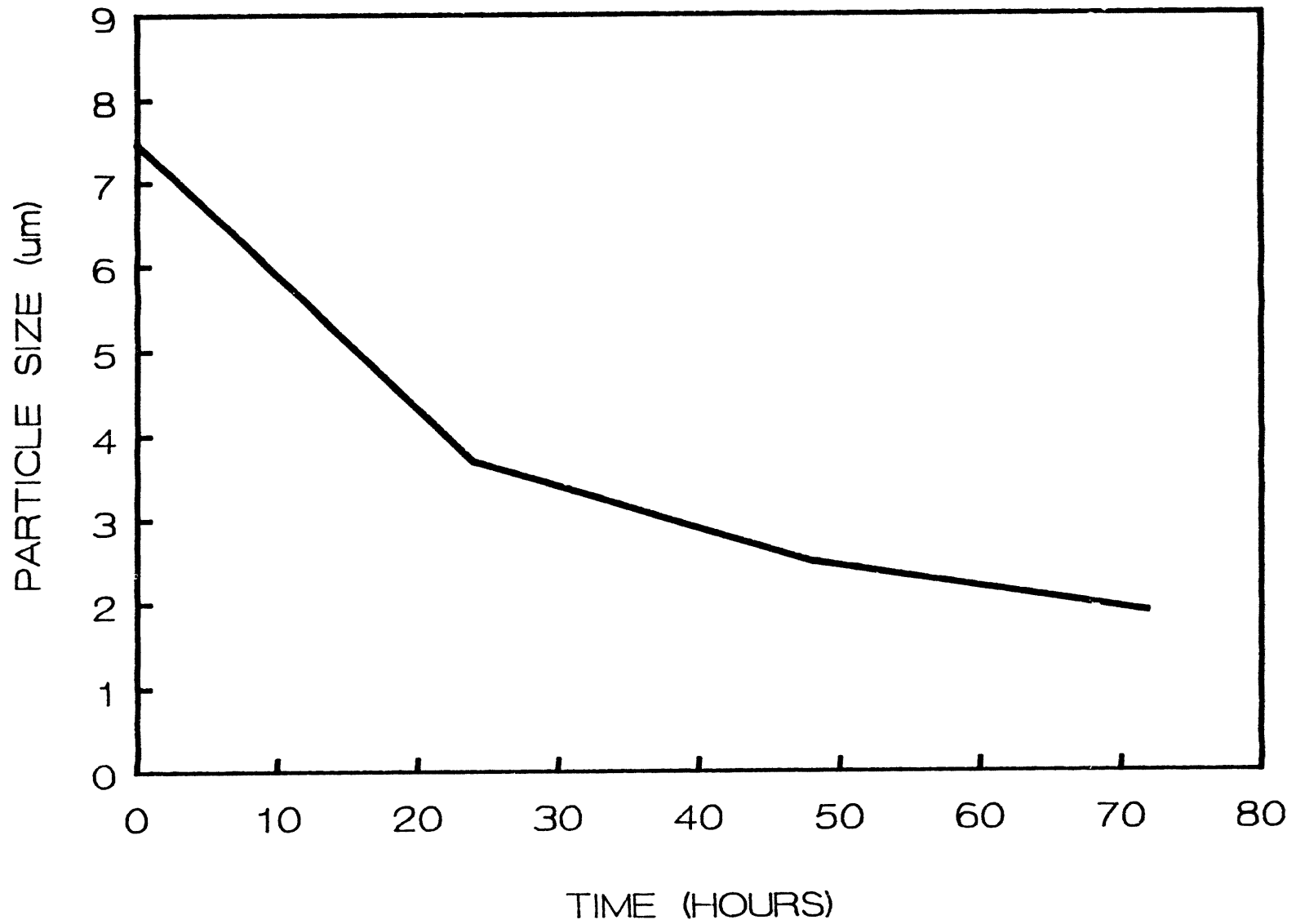
PRESSURE: 10 KPSI

MAGNIFICATION: 10,000 X

SAMPLE PREP: FRACTURE SURFACE

DATE: 06/01/91

LITHIUM ALUMINATE MILLING STUDY W/ 10% LITHIUM FLUORIDE

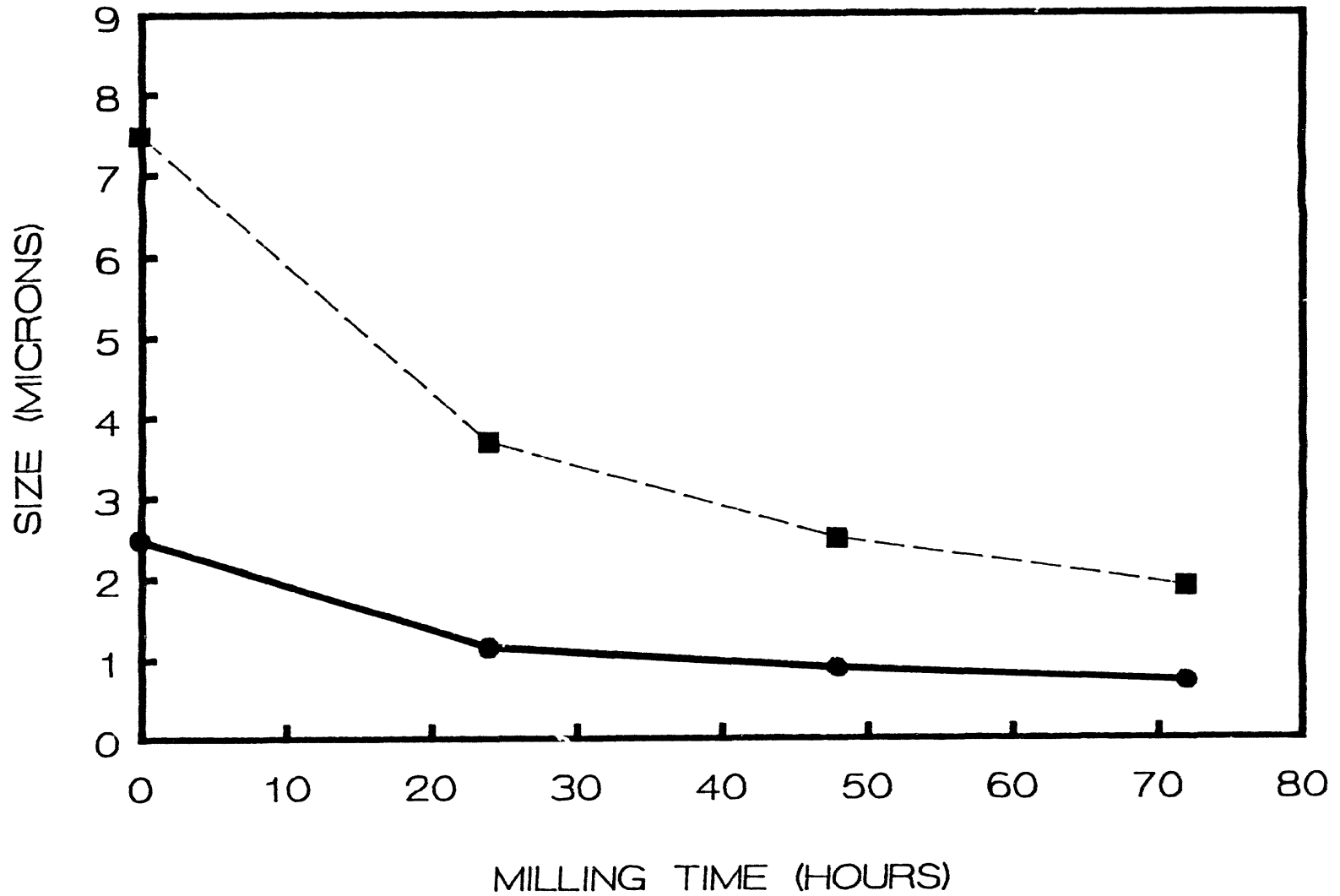


PORE & PARTICLE SIZE VS. MILLING TIME

LiAlO₂ & 10% LiF • 10KPSI/1300 C

—●— PORE DIA

-■- PARTIC DIA

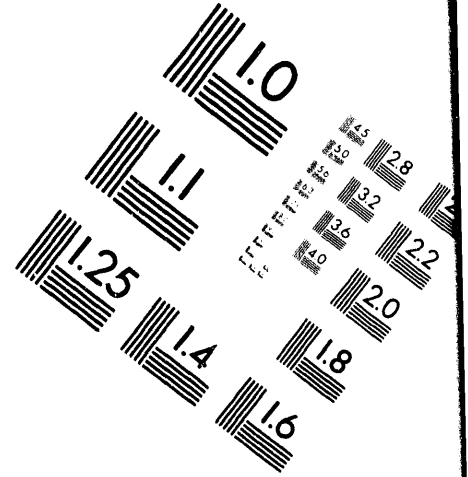
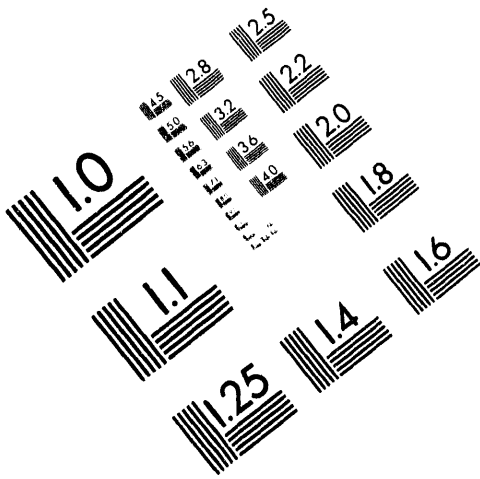




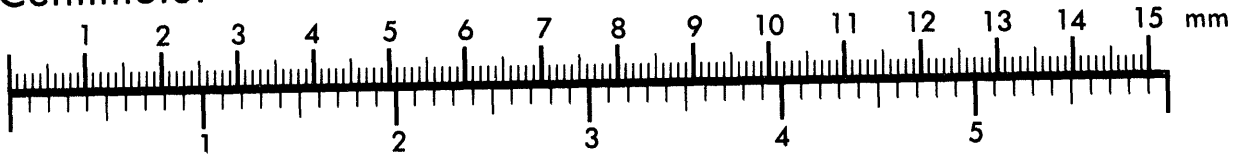
AIM

Association for Information and Image Management

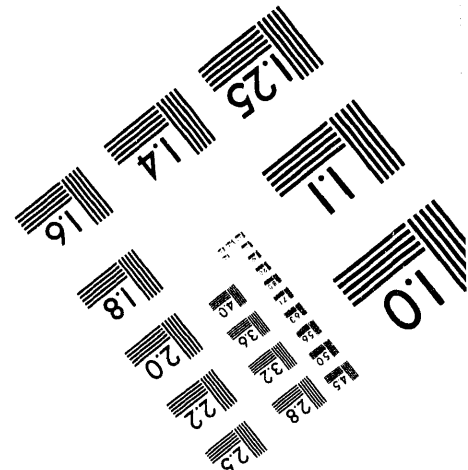
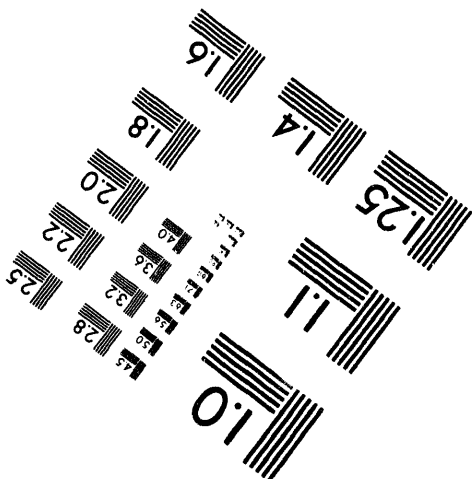
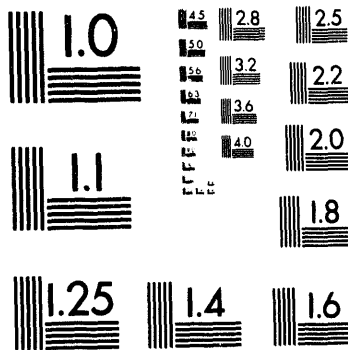
1100 Wayne Avenue, Suite 1100
Silver Spring, Maryland 20910
301/587-8202



Centimeter



Inches



MANUFACTURED TO AIM STANDARDS
BY APPLIED IMAGE, INC.

3 of 3

PARTICLE SIZE DISTRIBUTION

CI 2204

SAMPLE IDENTIFICATION *21 A1*

Density *2.55* g/cc LIQUID

Preparation

K-616 300g/L A-57 300g/L

Density g/cc Viscosity cp

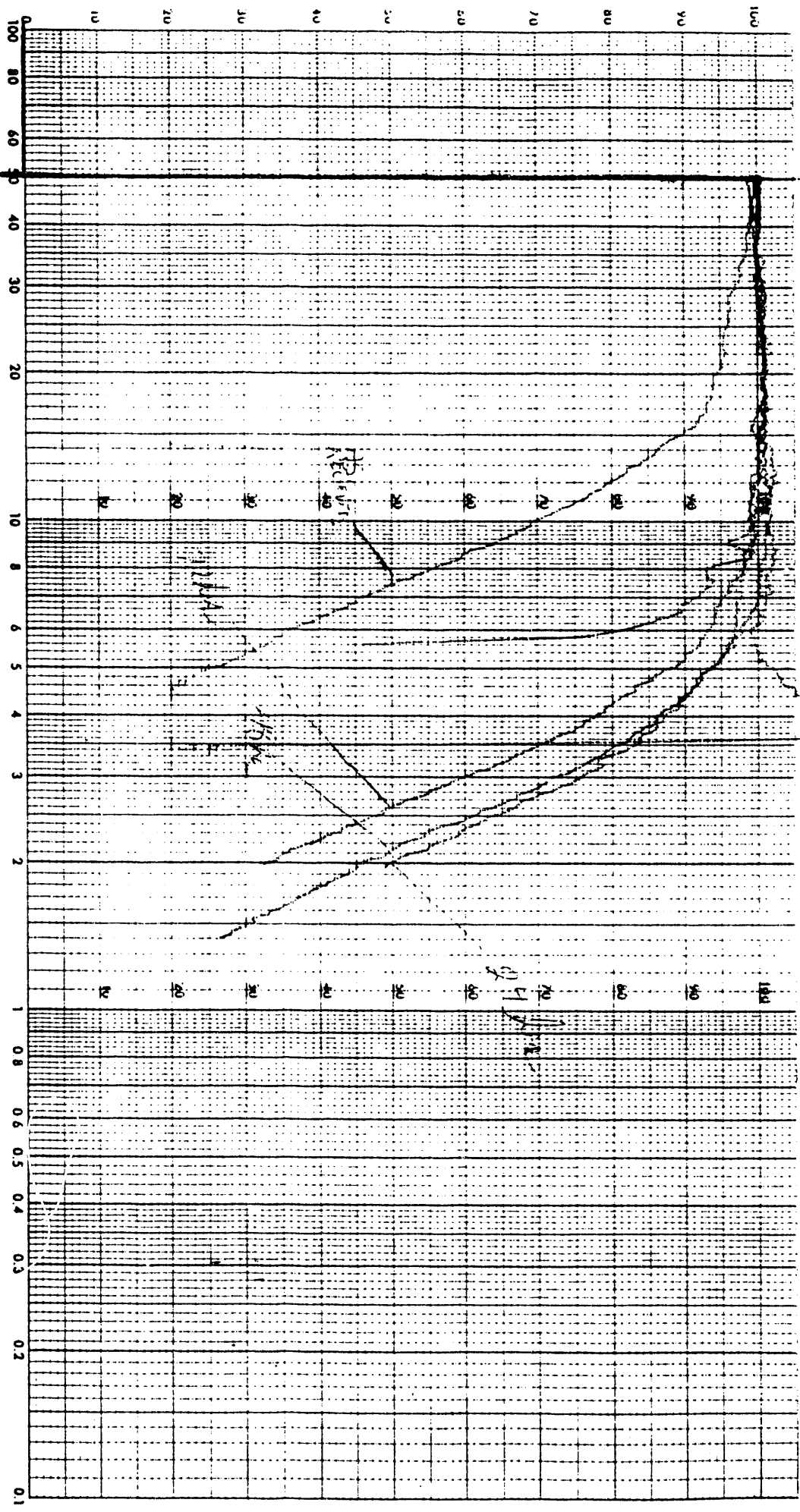
DATE *6-3-72*

BY *D. S. [Signature]*

TEMPERATURE *28* °C

RAIR *1/0-1* STAKT DIA *380* μm

CUMULATIVE PERCENT 67.1



EQUIVALENT SPHERICAL DIAMETER, μm

PARTICLE SIZE DISTRIBUTION

CL-2204

SAMPLE IDENTIFICATION *K: A1*

Density *2.558* g/cc LIQUID

Preparation *05 Adlex 270*

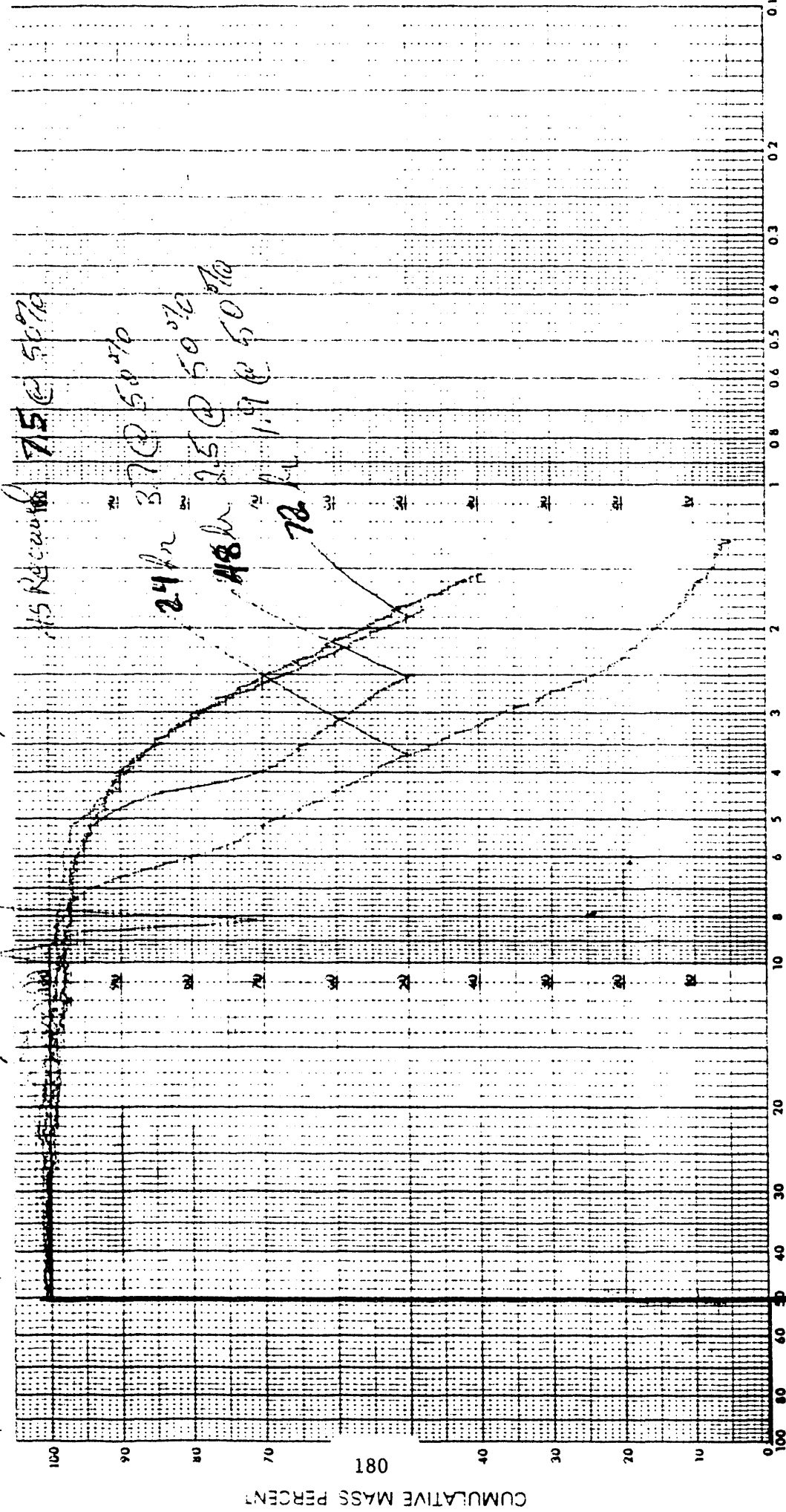
*15 min K-616 - 8.0%
K-57 - 6.0%
K-58 - 6.0%*

DATE *6-16-92*

BY *D. Hunt*

TEMPERATURE *28* °C

Humidity *45.4* % RH



EQUIVALENT SPHERICAL DIAMETER μm